Please cite the Published Version

R Camargo, J, Crapnell, RD, Bernalte, E, Janegitz, BC and Banks, CE (2025) Water-Based Conductive Ink for the Production of Carbon Black Screen-Printed Electrodes and the Detection of Tryptophan. ACS Applied Electronic Materials, 7 (12). pp. 5599-5610. ISSN 2637-6113

DOI: https://doi.org/10.1021/acsaelm.5c00550

Publisher: American Chemical Society (ACS)

Version: Published Version

Data Access Statement: The data will be available under requirement.

ACS APPLIED ELECTRONIC MATERIALS

pubs.acs.org/acsaelm Article

Water-Based Conductive Ink for the Production of Carbon Black Screen-Printed Electrodes and the Detection of Tryptophan

Jéssica R Camargo, Robert D. Crapnell, Elena Bernalte, Bruno C. Janegitz,* and Craig E. Banks*

Cite This: *ACS Appl. Electron. Mater.* 2025, 7, 5599−5610

Read Online

ACCESS | Metrics & More | Article Recommendations | Supporting Information

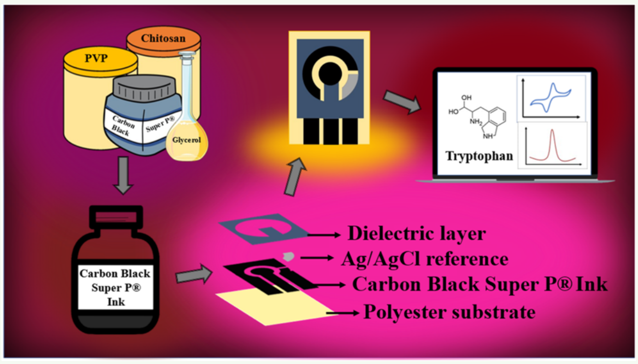

ABSTRACT: The development of versatile, cost-effective, and reproducible electrochemical sensors has gained importance due to their adaptability to specific applications through variations in composition and design. Water-based conductive inks have emerged as environmentally friendly alternatives to meet sustainability requirements and eliminate hazardous solvents. In this study, a screen-printed electrode (SPE) sensor utilizing a water-based conductive ink composed of Carbon Black Super P (CBSP), poly(vinylpyrrolidone) (PVP) and chitosan is presented. The ink formulation was optimized for a 5% CBSP composition, resulting in a homogeneous surface and superior reproducibility with a relative standard deviation of 7.99% ($n = 5$). The optimized sensor exhibited quasi-reversible behavior in cyclic voltammetry and an electroactive area 198.57% larger than its geometric area. The analytical performance for tryptophan detection showed a linear range from 0.5 to 300 μmol L^{-1} ($R^2 = 0.9946$), a limit of detection of 0.018 μmol L^{-1}, and interference rates below 10% for common compounds. The recovery rates for pharmaceutical and beverage samples ranged from 86.2% to 114%. The sustainable design, excellent sensitivity, and cost-effective manufacturing make this SPE sensor a robust tool for point-of-use tryptophan quantification.

KEYWORDS: *screen-printed, electrochemical sensor, carbon black super P, conductive water-based ink, tryptophan*

1. INTRODUCTION

The development of disposable, portable, and easy-to-use sensors is promising, since these electrochemical devices are relatively inexpensive and have good sensitivity and limits of detection (LOD) comparable to expensive technologies.[1] In this sense, such devices can be portable, disposable, wearable, or flexible,[2−4] which increases their applicability for *in vivo* and real-time detection of clinical, pharmaceutical, or pollutant analytes.[5] Electroanalysis is particularly suited for in situ monitoring; however, classical electrodes are limited by high cost, frequent polishing, and complex maintenance requirements. Screen-printed electrodes (SPEs) offer a cost-effective alternative, enabling mass production with minimal pretreatment and scalable economic advantages.[6] However, the single-use and disposable nature of most SPEs raises concerns about their sustainability. The disposal and waste management of these electrodes, often made on plastic substrates for single-use, could exacerbate plastic pollution. In this sense, developing sustainable manufacturing and effective recycling methods is crucial to address these environmental challenges.[6] From a sustainability perspective, these sensors contribute to reducing environmental impact when constructed using eco-friendly materials, such as water-based conductive inks and renewable substrates, which are in line with the principles of green chemistry and the circular economy.[7,8]

Screen-printed electrodes (SPEs) are systems developed from conductive ink on inert substrates and are characterized by portability, low cost, and ease of use.[9] Their configuration as miniaturized electrochemical cells, using small volumes for measurements, has increased their relevance.[10,11] Additionally, SPE technology enables different designs and sizes, ideal for real-time and on-site analyses.[12,13] The production of SPEs requires screens with sufficient porosity to allow the ink to penetrate and adhere to substrates such as paper, plastic or ceramic, which must resist curing temperatures and solvents.[14−17] The ink is applied uniformly across the mesh using a squeegee, creating a conductive layer on the substrate.[18] By combining polymers, solvents, and conductive materials, conductive inks can be tailored to improve electrochemical sensor performance.[19,20] Most commercially available SPEs

Received: March 20, 2025
Revised: May 28, 2025
Accepted: May 29, 2025
Published: June 4, 2025

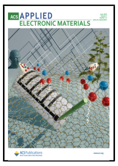

rely on organic solvent-based conductive inks, which pose sustainability challenges due to their environmental impact, including the release of volatile organic compounds (VOCs) that contribute to air pollution and health hazards.

The adoption of water-based conductive inks aligns with the goals of reducing VOCs and promoting safer, more sustainable manufacturing processes.[21] Using biopolymers like chitosan enhances biodegradability while maintaining effective adhesion properties in water-based inks, making them suitable for environmentally friendly sensor production.[22] Chitosan improves adhesion by forming hydrogen bonds and ionic interactions with the substrate, replacing synthetic, non-biodegradable binders often derived from petroleum-based resins. Chitosans are a group of biopolymers whose physicochemical properties vary depending on factors such as molecular weight and the degree of acetylation or deacetylation.[23] Being zwitterionic, their behavior is strongly influenced by pH, which affects their solubility, charge distribution, and interaction with other materials.[24] These characteristics can be tuned to optimize performance in different ink formulations. Additives such as plasticizers and metal complexes enhance adhesion and amplify signals. Plasticizers improve SPE adhesion by increasing ink flexibility, preventing cracks, and enhancing flowability. Metal complexes amplify signals by boosting electrocatalytic activity and providing more active sites for electron transfer. In this sense, advances in material synthesis are improving SPE systems by introducing conductive inks with better homogeneity and substrate adhesion, enhancing conductivity and selectivity.[25,26] Carbonaceous materials are particularly suitable due to their availability, low cost, and diverse structures such as graphite, graphene, carbon black (CB), and nanotubes, which can be functionalized for improved properties.[27−30] Carbon black (CB), an inexpensive, highly conductive material with a large electroactive area, is ideal for conductive ink preparation.[31,32] Its stable dispersion eliminates the need for additional treatments.[33] CB modified with Super P (CBSP), an additive that optimizes electron transfer, has shown its potential in various applications, including lithium-ion batteries[34] and electrochemical sensors for macrolide antibiotics.[35]

The sustainability of SPEs is becoming increasingly important, with the need for eco-friendly materials driving innovation in ink formulations. Low-cost, biodegradable polymers such as chitosan, derived from chitin, offer significant advantages for sustainable conductive inks due to their biocompatibility, biodegradability, and excellent film-forming properties.[27,36−42] Studies by Phillips et al.[43] and Camargo et al.[34] have demonstrated the compatibility of chitosan and Poly(vinylpyrrolidone) (PVP) with carbon black (CB), enhancing the performance of SPE systems. Chitosan serves as an ideal binder, while PVP improves ink uniformity and stability by reducing surface tension and preventing agglomeration of conductive particles.[44] A water-based ink combining PVP, chitosan, glycerol, and CB, used in SPEs, not only contributes to environmental sustainability but also offers better performance in terms of stability, conductivity, and electrochemical consistency compared to traditional methods.

Tryptophan (TRP), a biomarker that influences human biochemical and physiological responses, is widely used as a sleep aid, appetite suppressant, and antidepressant.[45−47] It is also effective against headaches and obesity,[48] which makes its detection in food, pharmaceuticals, and biological samples valuable. However, the detection of TRP is associated with challenges: degradation in acidic media or complications due to oxygen evolution in alkaline conditions.[49,50] Although HPLC is a reliable method, it is expensive and slow.[51] Electroanalytical methods offer cheaper and faster alternatives without compromising efficiency. This work aims to develop and investigate an SPE system using a new conductive water-based ink with CBSP in a PVP-chitosan polymer matrix for TRP detection. This approach provides a low-cost, sensitive, and efficient platform for the quantification of TRP in various samples.

2. EXPERIMENTAL SECTION

2.1. Chemicals. The reagents used to prepare the ink and to prepare the supporting electrolyte solutions, electrochemical probes and other samples were all of analytical grade and were purchased from Fisher or Sigma-Aldrich. The solutions were prepared with purified water using the Milli-Q Integral 3 system from Millipore UK (Watford, U.K.) (resistivity ≥ 18.2 MΩ cm). In the measurements performed for the electrochemical characterization of the sensors made, 0.1 mol L^{-1} KCl solution was used as electrolyte supporting an equimolar mixture of potassium ferricyanide (99%), potassium ferrocyanide (98.5−102%), or Hexaammineruthenium(III) chloride (RuHex, 98%) and Ferrocenemethanol as electrochemical probes. The phosphate-buffered saline (PBS) tablets were purchased from Merck (Gillingham, U.K.). Carbon black (Super P, > 99+%) was purchased from Fisher Scientific (Loughborough, U.K.). The droplet volume used on the sensor was 40 μL. Real samples of pharmaceutical EPAPLUS and the food samples, whole milk Longlife (Tesco) and Apple juice (Naturis) were obtained from local convenience stores.

2.2. Samples. The samples used for TRP determination included pharmaceutical TRP tablets and fortified beverages such as apple juice and cow's milk. The tablets were crushed to obtain a homogeneous powder and then dissolved in a buffer solution until the desired concentrations. The beverages were mixed with the buffer and controlled aliquots of TRP were added to this solution for subsequent analyses.

2.3. Equipment. A Metrohm Autolab PGSTAT M204 Metrohm Potentiostat/Galvanostat controlled by Nova 2.1.6 software was used for electrochemical analyzes. The connector developed by ADB sensores was used to connect the electrochemical system to the potentiostat. Scanning electron microscopy (SEM) analysis was performed using a Crossbeam 350 Focused Ion Beam—Scanning Electron Microscope (FIB-SEM) (Carl Zeiss Ltd., Cambridge, U.K.) equipped with a field emission electron gun. Imaging was performed using a secondary electron secondary ion (SESI) detector. Samples were attached to the aluminum pins of the SEM using self-adhesive carbon tabs (12 mm diameter, Agar Scientific, Essex, U.K.). Raman spectroscopy was performed using a Renishaw PLC in a Raman microscope controlled by WiRE 2 software at a laser wavelength of 514 nm. The contact angle measurements was performed using the equipament developed by Silva.[52] FTIR analysis was performed using a Bruker TENSOR II spectrophotometer (Ettlingen, Baden-Württemberg, Germany) in transmittance mode, covering the spectral range from 400 to 4000 cm^{-1} with a resolution of 1.0 cm^{-1}.

2.4. Preparation of Screen-Printed Electrodes (SPE). Stencils for a microDEK1760RS screen printing machine (DEK, Weymouth, United Kingdom) were used to produce the SPE sensors. In this way, the water-based conductive CBSP ink was optimized for the desired application. The polymer solution was prepared using 1.0 g of PVP, 1.0 g of chitosan and 50 mL of a 2% acetic acid solution mixed for 2h with the aid of a stirrer. The preparation of the conductive ink was carried out using a stirrer. The best ratio between CBSP and the PVP-chitosan polymer solution was chosen to achieve a higher conductivity of the finished electrode. The number of times the squeegee over the screen was performed to get a homogeneous surface of the carbon ink. The ink was then screen-printed onto a polyester substrate and each layer was dried at 60 °C for 30 min. After the conductive CBSP ink, an Ag/AgCL paste (SunChemical) was used to make the reference

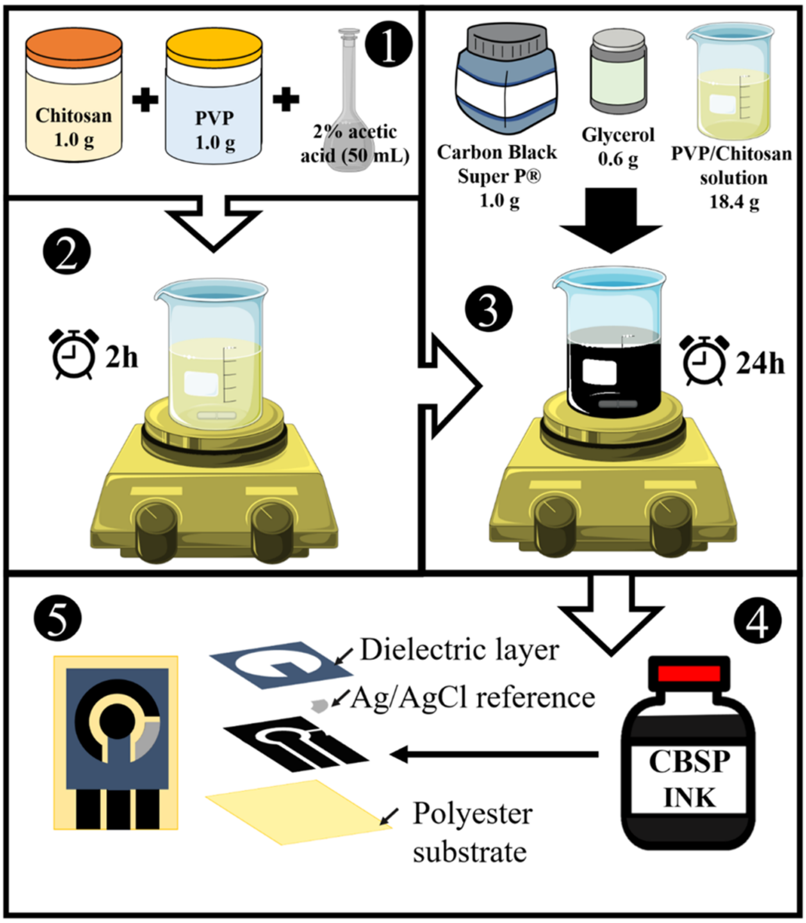

Figure 1. Scheme of SPE preparation using the CBSP ink. (1) To create the polymer solution, 1.0 g of PVP, 1.0 g of Chitosan, and 50 mL of a 2% acetic acid solution were used, (2) The mixture was mixed for 2 h with the assistance of a stirrer. (3) To create the ink CBSP, 1.0 g of CBSP, 0.6 g of glycerol and 18.4 g of the polymer solution were mixed for 24 h with the assistance of a stirrer. (4) The ink was ready to be used. (5) the screen-printing machine was used to perform the SPE system, the squeegee was passed over the screen three times to ensure an even surface for the carbon ink. This carbon ink was applied to a polyester substrate and dried at 60 °C for 30 min. Ag/AgCl paste was then applied to form the reference electrode layer and dried at 60 °C for 30 min. To define the three electrodes and delineate the sample area, a dielectric ink was used to cover the terminals. The finished sensor was dried at 60 °C for 12 h to ensure it was ready for use.

electrode layer and to delimitate the three electrodes and define the sample area, a dielectric ink (SunChemical) was used to cover the terminals. The final sensor was dried at 60 °C for 12h and it was ready to be used, see Figure 1.

3. RESULTS AND DISCUSSION

3.1. Production of Carbon Black Water-Based Ink and SPE System. To produce the ink, it was first necessary to test how the polymer powder dissolves in an aqueous solution. Compositions containing only PVP and water resulted in a low-viscosity solution that favored a complete distribution of the ink over the screen without respecting the mesh patterns. It is known from previous work that chitosan allows the formation of ideally viscous solutions for the development of ink. In this sense, different solutions were prepared with PVP and chitosan in the same ratio. The ratio of 1.0 g PVP, and 1.0 g chitosan in 50 mL of a 2% acetic acid solution was the mixture that had sufficient viscosity to allow the addition of CBSP and not percolate through the screen mesh. The addition of small amounts of glycerol improves the adhesion and homogeneity of the ink, so the amount of 3% is maintained for all subsequent studies.

After the polymer solution and the amount of glycerol were determined, the amount of CBSP in the ink composition was tested. Three ink compositions with 3, 5, and 7% CBSP were tested (see Figure 2A). The inks with 3 and 5% CBSP were homogeneous, but it should be noted that the electrode made with the ink containing 3% CBSP did not show homogeneity in screen-printing. The lack of homogeneity is also evident in the cyclic voltammetry tests carried out for five of these devices, see Figure S1. In the 7% composition, the presence of agglomerates can be observed, which shows that this composition was not homogeneous. These agglomerates also hindered the screen-printing process. The composition that showed homogeneous and complete substrate coverage during application was 5% CBSP. It also showed good reproducibility with a relative standard deviation of 7.99% $n = 5$.

After the composition of the ink was finalized, the number of passes of the squeegee over the screen was examined. One, two and three times of ink applications were tested, see Figure 2B. Electrochemical changes, including increased capacitive current and broader peak-to-peak separation, were observed with additional squeegee passes, indicating a thicker ink layer and altered interfacial properties. However, the efficiency in producing visually homogeneous sensors was much greater

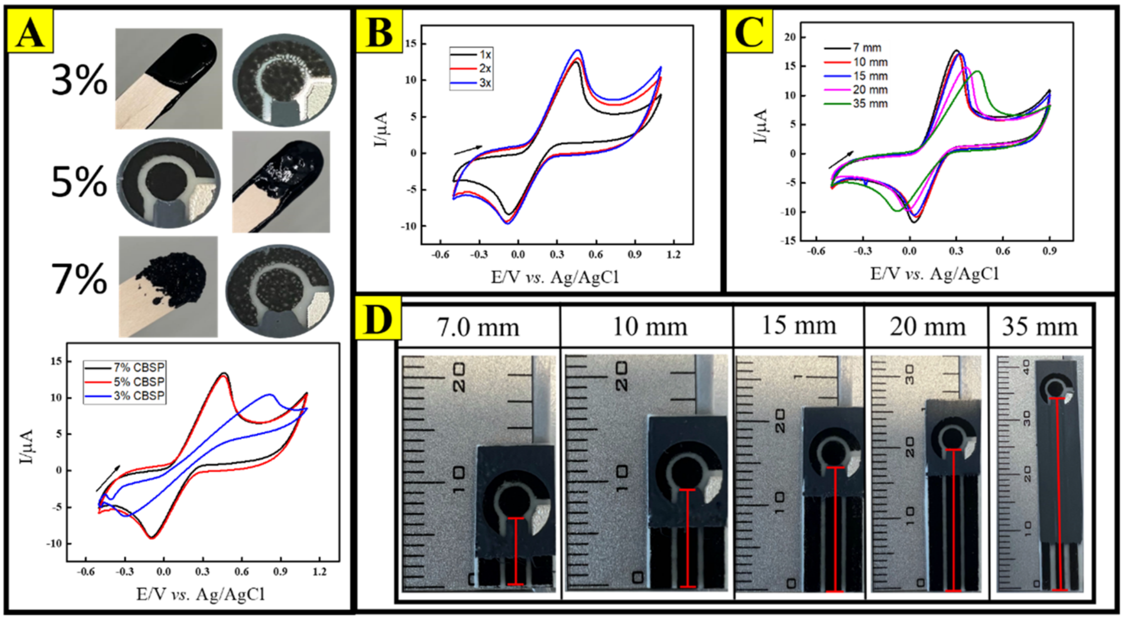

Figure 2. (A) Photos of different percentages of CBSP ink and CBSP-PVP-CH/PES systems and Cyclic voltammogram obtained by CBSP-PVP-CH/PES with varying percentages of CBSP (3, 5 and 7%) in 0.1 mol L^{-1} KCl and 1.0 mmol L^{-1} ferrocenemethanol, ν = 50 mV s^{-1}; (B) Cyclic voltammograms obtained by CBSP-PVP-CH/PES comparing different times pass the squeegee over the screen (1×, 2× and 3×), in 0.1 mol L^{-1} KCl and 1.0 mmol L^{-1} ferrocenemethanol, ν = 50 mV s^{-1}; (C) Cyclic voltammograms of CBSP-PVP-CH/PES comparing different tail length, in 0.1 mol L^{-1} KCl and 1.0 mmol L^{-1} ferrocenemethanol, ν = 50 mV s^{-1}; (D) Images of different tail length 7.0, 10.0, 15.0, 20.0, and 35.0 mm.

when the squeegee was run three times. See the study for five electrodes in the Supporting Information Figure S2.

The screen used to produce the sensors had a tail length of 35 mm. However, by seeking to improve the analytical signals by reducing the resistance, we can shorten the manufactured system.[53] With this in mind, systems with tail lengths of 7.0, 10.0, 15.0, 20.0, and 35.0 mm were tested. The measurements were carried out with a caliper. As expected, the electrodes with the shortened lengths 7.0, 10.0, and 15.0 mm showed a higher current than those with 20.0, and 35.0 mm. Therefore, a length of 10 mm was chosen to continue the work, see Figure 2C,D.

Using the methodology described in item 2.4, PVP chitosan, glycerol and CBSP sensors were manufactured, which were deposited on polyester and this device was named CBSP-PVP-CH/PES. Images of the finished sensors are shown in Figure 3.

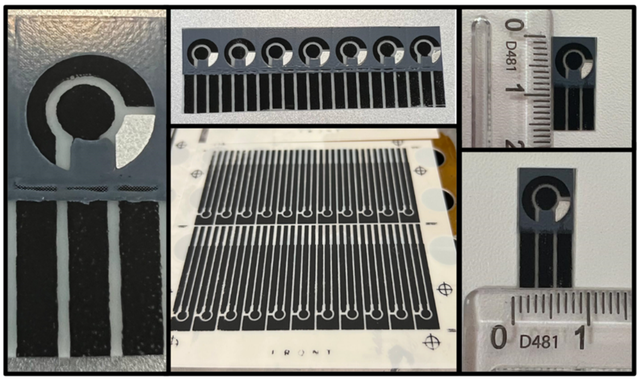

Figure 3. Pictures of disposable sensing systems prepared using PVP-chitosan, glycerol and CBSP applied on polyester, with 16.0 mm (length) × 8.0 mm (width). This device was named CBSP-PVP-CH/PES.

SEM analysis, see Figure 4(A–D), was performed to elucidate the microstructural composition of the ink containing CBSP, Chitosan, and PVP. The images obtained provide valuable insights into the morphology and interfacial properties of the composite ink. The microscopic images show a well-dispersed distribution of CBSP particles throughout the ink matrix. The spherical and irregular morphology of CBSP is evident and shows that it has been successfully integrated into the ink formulation. In addition, chitosan and PVP contribute to the overall structure and appear as a continuous matrix that encapsulates and interacts with the CBSP particles. The SEM images suggest a homogeneous mixture of the components, indicating effective compatibility and dispersion within the ink. The presence of chitosan and PVP appears to influence the surface properties and contribute to a smoother microstructure.

The Raman measurement, see Figure 4E, shows characteristic bands at 1589 and 1350 cm^{-1} that are likely associated with specific vibrational modes or features in CBSP. The band at 1589 cm^{-1} often corresponds to the G-band in carbon materials such as graphene and carbon nanotubes.[54] The G-band typically represents the stretching vibration of the sp^2-hybridized carbon atoms in a two-dimensional lattice structure.[55] The presence of this band indicates the graphitic nature of the CBSP material. The 1350 cm^{-1} band is usually associated with the D-band in carbon materials, which indicates structural defects or disorders in the carbon lattice.[55] The presence of this band may indicate imperfections or disordered areas within the CBSP ink.

Through electrochemical impedance spectroscopy (EIS) analysis, the Nyquist diagram shows a small semicircle followed by another semicircle and a Warburg element, that indicates a system with multiple electrochemical processes. The small semicircle represents a fast-kinetic process, possibly related to the initial stages of charge transfer. The larger semicircle

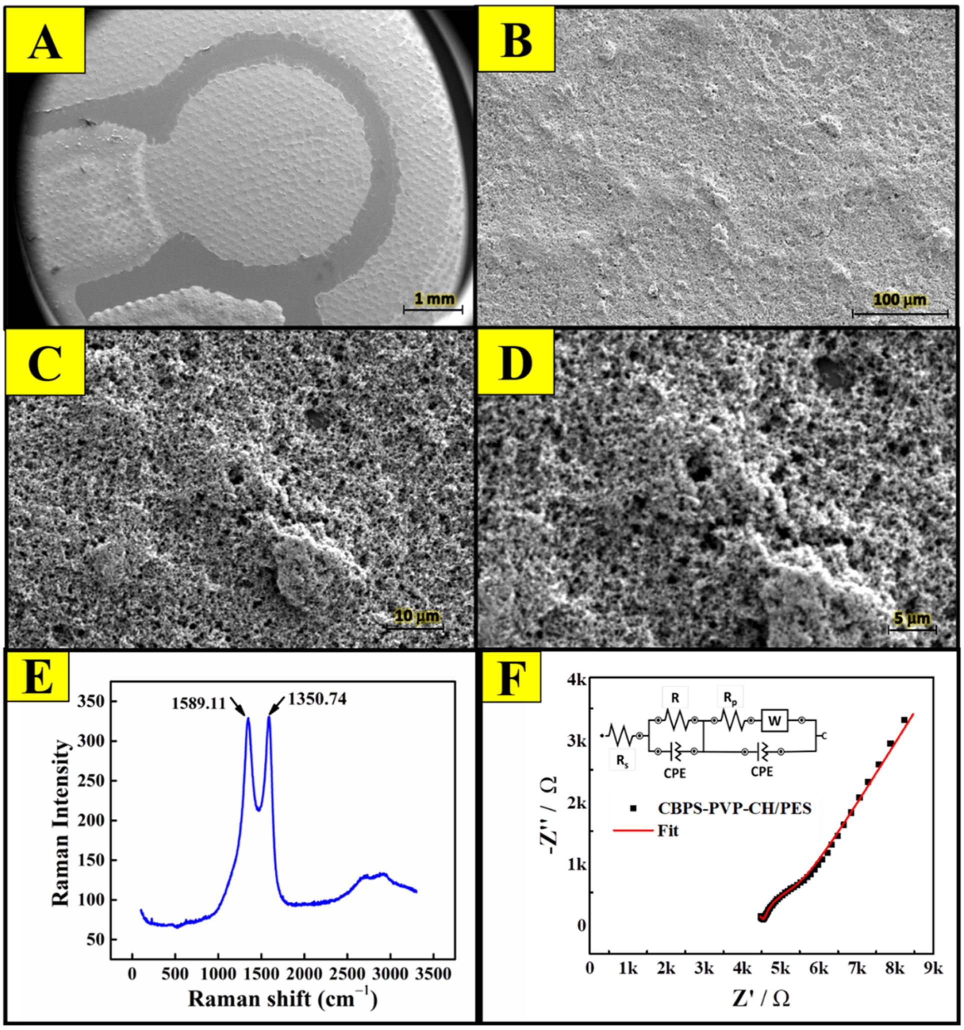

Figure 4. Composite ink microstructure observed through Scanning Electron Microscopy (SEM). CBSP particles are uniformly dispersed within a chitosan and PVP matrix, showcasing a homogeneous and porous structure (A) SEM images obtained for CBSP-PVP-CH/PES at 31× magnification; (B) 500×; (C) 3000×; (D) 5000×; (E) Raman spectroscopy of CBSP-PVP-CH/PES sensor; (F) Nyquist diagrams for CBSP-PVP-CH/PES in 1.0 mmol L^{-1} ferrocenemethanol in 0.1 mol L^{-1} KCl, E = 130 mV. Inset: [R(RQ)([RW]Q)] equivalent circuit.

indicates a slower electrochemical process, possibly involving another electrochemical reaction, and the Warburg element indicates a diffusion-controlled process in which the movement of ions contributes to the impedance response. The Nyquist plots obtained through electrochemical impedance spectroscopy in ferrocenemethanol (1.0 mmol L^{-1}, 0.1 mol L^{-1} KCl) and the equivalent circuit were presented in Figure 4F. In addition to the electrochemical characterizations, the Supporting Information also includes the Nyquist plots for sensors with varying tail lengths (7, 10, 15, 20, and 35 mm, Figure S5).

The contact angle analysis was used to assess the wettability of the different surfaces involved in sensor fabrication. Figure 5A, consisting solely of the conductive ink, exhibited the lowest contact angle, indicating a more hydrophilic surface. This property is beneficial for electrochemical sensors, as it promotes better spreading of the electrolyte droplet and enhances the interaction between the analyte and the electrode. Figure 5B, corresponding to the bare substrate, showed a significantly higher contact angle, characterizing it as a hydrophobic surface. This feature can be advantageous for defining the sensor's active area, helping to confine the liquid sample and prevent undesired spreading. Finally, sample Figure 5C, representing the fully assembled sensor, presented an intermediate behavior, reflecting a balance between the ink's hydrophilic nature and the substrate's hydrophobic characteristics. This equilibrium is crucial for ensuring both efficient sample retention within the active region and effective electrochemical transduction.

The Fourier-transform infrared (FT-IR) spectroscopy analysis of the composite ink comprising carbon black Super P, chitosan, and poly(vinylpyrrolidone) (PVP), reveals distinct absorption bands corresponding to the functional groups of chitosan and PVP. Carbon black, being predominantly graphitic, exhibits minimal IR activity. A broad absorption band around 3400 cm^{-1} is indicative of O−H and N−H stretching vibrations, characteristic of chitosan's hydroxyl and amine groups.[56] This band also suggests the presence of hydrogen bonding interactions within the composite. The C−H stretching vibrations observed near 2900 cm^{-1} are attributed to the aliphatic chains in both chitosan and PVP.[56,57] The prominent absorption band at approximately 1650 cm^{-1} corresponds to the C−O stretching vibration of the amide group in PVP, confirming its incorporation into the composite.[57] Additionally, the band near 1550 cm^{-1} is

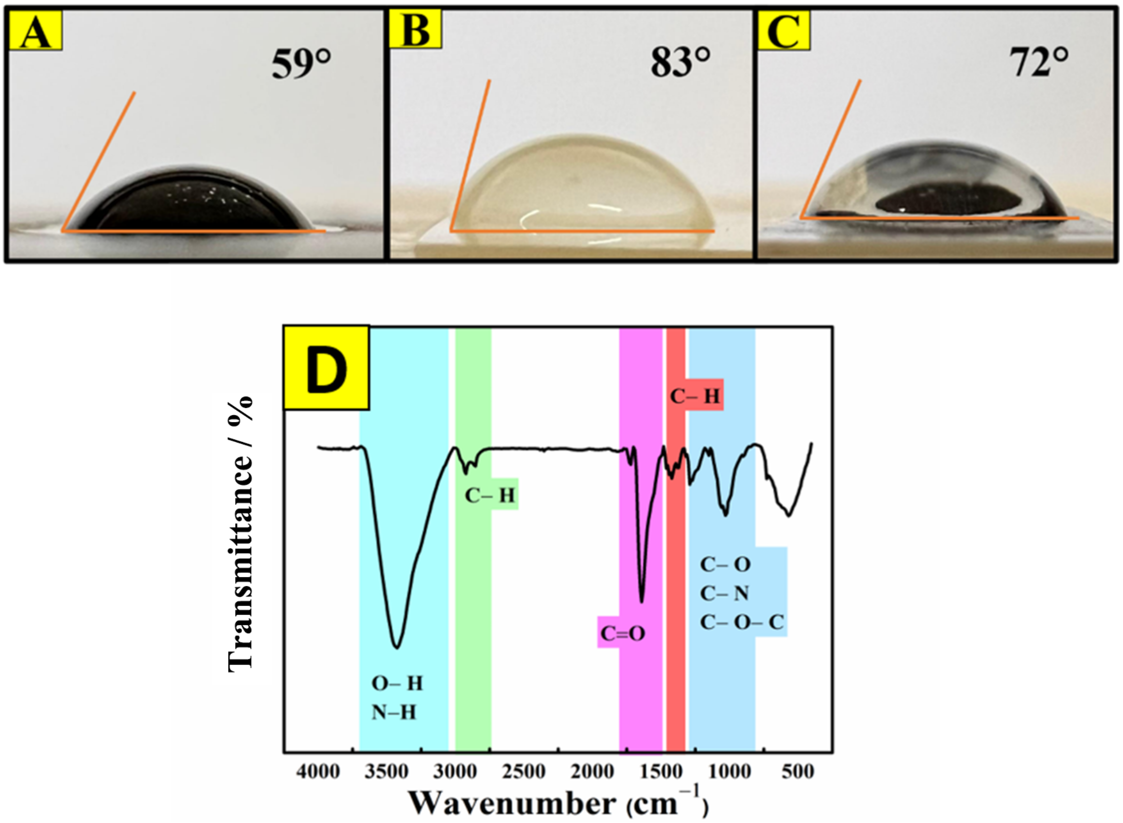

Figure 5. Water contact angle measurements for (A) the conductive ink, (B) the substrate, and (C) the complete printed sensor; (D) FT-IR spectrum of the conductive ink containing carbon black Super P, chitosan, and PVP.

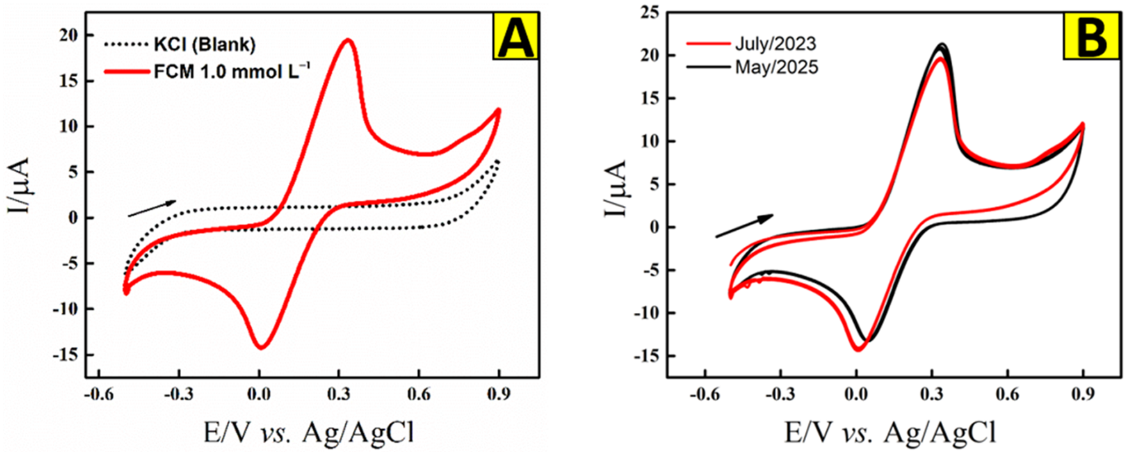

Figure 6. (A) Cyclic voltammograms performed in 0.1 mol L^{-1} KCl in the presence of 1.0 mmol L^{-1} ferrocenemethanol. Scan rate = 50 mV s^{-1}. (B) Cyclic voltammograms of CBSP-PVP-CH/PES electrodes measured in July 2023 (red) and May 2025 (black), performed in 0.1 mol L^{-1} KCl in the presence of 1.0 mmol L^{-1} ferrocenemethanol. Scan rate = 50 mV s^{-1}.

associated with N−H bending vibrations, further supporting the presence of chitosan. The region between 1200 and 1000 cm^{-1} exhibits bands related to C−O and C−N stretching vibrations, common to both chitosan and PVP.[58] These spectral features collectively confirm the successful integration of chitosan and PVP within the composite conductive ink matrix, see Figure 5D.

Therefore, to initiate the electrochemical characterization of the manufactured ink, the CBSP-PVP-CH/PES device underwent cyclic voltammetry. A solution of ferrocenemethanol (1.0 mmol L^{-1}, 0.1 mol L^{-1} KCl) was utilized at a scan rate of 50 mV s^{-1}. An anodic peak of 19 μA at 0.33 V and a cathodic peak of −14 μA at 0.01 V can be observed (Figure 6A). The calculated Ia/Ic ratio is 1.35, and the peak-to-peak separation corresponds to 326 mV. The peak potential separation of 326 mV indicates the quasi-reversible nature of the redox process. A stability analysis was conducted using sensors fabricated in 2023 and re-evaluated after 23 months in 2025. The sensors were stored in heat-sealed plastic packaging at room temperature. Over this period, only a ∼ 7% variation was observed in the oxidation and reduction peak currents, despite the analyses being carried out in different laboratories

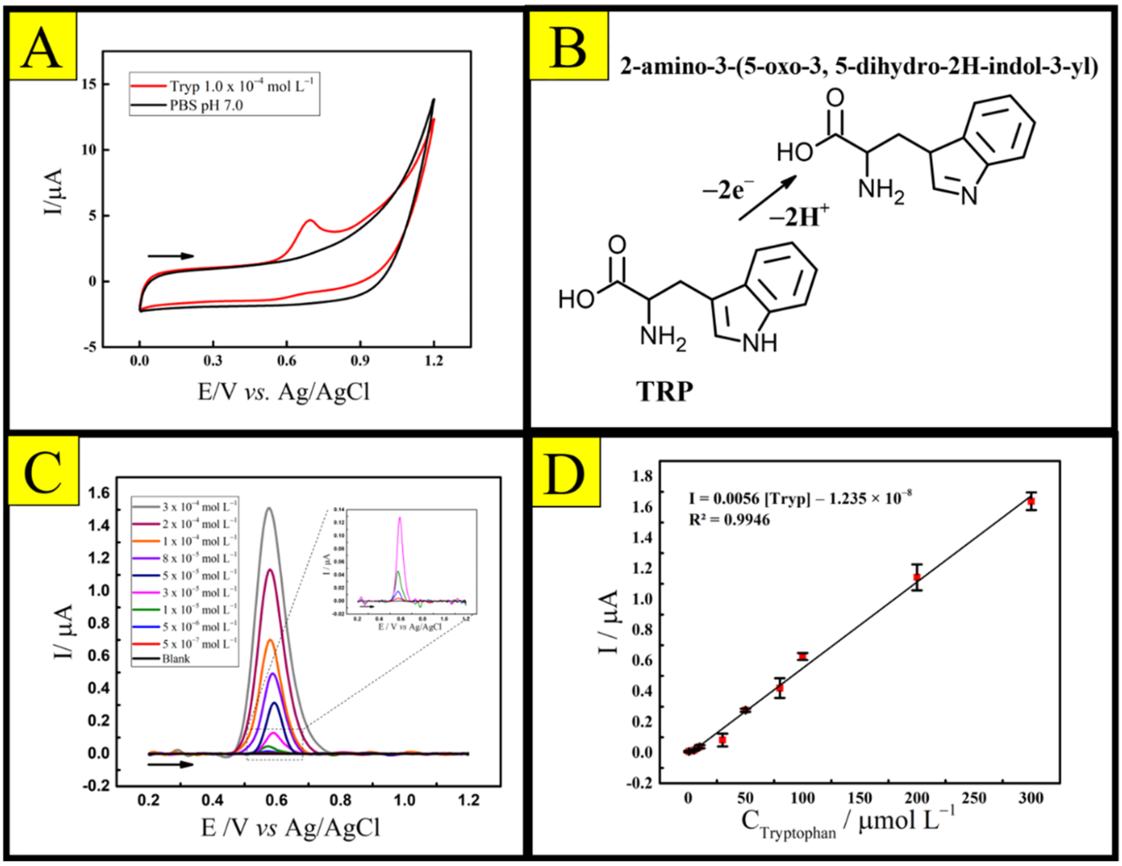

Figure 7. (A) Cyclic voltammograms obtained with CBSP-PVP-CH/PES in the absence and presence of 100 μmol L^{-1} TRP. Supporting electrolyte: 0.10 mol L^{-1} phosphate buffer solution (pH 7.0). ν = 50 mV s^{-1} (B) Electrochemical oxidation mechanism of TRP; (C) Differential pulse voltammograms in the presence of TRP at concentrations of 0.5, 5.0, 10.0, 30.0, 50.0, 80.0, 100.0, 200.0, and 300.0 μmol L^{-1} in phosphate buffer 0.1 mol L^{-1} (pH 7.0); (D) Graph of points obtained through the analytical curve for TRP.

(Manchester, U.K., in 2023 and Araras, Brazil, in 2025) using independently prepared electrolyte solutions. This minimal change, combined with the preservation of very similar voltammetric profiles, supports the robustness and long-term stability of the sensor system, see Figure 6B.

The electrochemical active area of the CBSP-PVP-CH/PES electrode (Figure S3) was estimated based on the Randles−Ševčik equation[59] (eq 1) at scan rates ranging from 5.0 to 100 mV s^{-1} using 1.0 mmol L^{-1} ferrocenemethanol as a probe in a 0.1 mol L^{-1} KCl solution:

Equation 1, Randles−Ševčik

$$I_p = \pm 2.69 \times 10^5 n^{3/2} A C D^{3/2} v^{1/2} \tag{1}$$

Where I_p is the peak current, n is the number of electrons in the reaction, A refers to the value of the electroactive area, C is the concentration of the redox probe, D is the diffusion coefficient of the probe and v is the scan rate. The slope of the I_{pa} vs $v_{1/2}$ of the cyclic voltammograms were recorded at different scan rates in 1.0 mmol L^{-1} ferrocenemethanol as a probe in a 0.1 mol L^{-1} KCl to estimate A, see Figure S3. The diffusion coefficient D is the diffusion coefficient of the electroactive species ($D = 7.6 \times 10^{-6}$ cm^2 s^{-1}) and v is the scan rate. The average electrochemically active area obtained from the anodic and cathodic currents was (0.139 ± 0.02) cm^2. The geometric area of the electrodes is 0.07 cm^2 for the working electrode. Using the following eq 2

$$\%\mathrm{Real} = (A_{real}/A_{geo}) \times 100 \tag{2}$$

the % Real is 198,57%, which means that the electroactive area obtained was 2 times greater than the geometric area.

3.2. Determination of Tryptophan. Cyclic voltammetric measurements in the absence and presence of 100 μmol L^{-1} TRP from 0.0 and 1.2 V, with a scan rate of 50 mV s^{-1} were obtained in 0.10 mol L^{-1} phosphate buffer solution (pH 7.0), see Figure 7A. The CBSP-PVP-CH/PES electrode showed an irreversible redox process, attributed to the oxidation of TRP to 2-amino-3-(5-oxo-3,5-dihydro-2*H*-indol-3-yl) propionic acid through a two-electron transfer process [6], as illustrated in Figure 7B.

Tryptophan possesses multiple ionizable groups, with pK_a values around 2.4 (carboxylic acid), 9.4 (amine), and approximately 16 (indole NH), which define its speciation across different pH levels.[60] These protonation states influence not only its solubility and stability but also its redox behavior at the electrode surface. In electrochemical detection, the pH of the supporting electrolyte governs the oxidation potential and peak current of TRP, with near-neutral pH (e.g., PBS pH 7.0) offering a balance between minimizing degradation in acidic media and avoiding oxygen evolution in basic conditions.The investigation into the effects of parameters on Differential Pulse Voltammetry (DPV) is important to obtain a higher analytical signal. This study involves an examination of key parameters such as modulation amplitude, interval time or scan rate, and modulation time to comprehend their influence on

Table 1. Determination of TRP in Pharmaceutical and Food Samples Using the CBSP-PVP-CH/PES by DPV Technique (n = 3)[a]

sample	solubilized tablet concentration (μmol L^{-1})	added (μmol L^{-1})	detected (μmol L^{-1})	recovery (%)
epaplus	5	-	4.57 (±0.65)	91.40 (±13.0)
	50	-	53.53(±2.78)	107.06(±5.57)
	200	-	227.7(±12.7)	113.89(±6.34)
apple juice	-	10	8.75 (±0.46)	87.47(±4.56)
	-	30	30.31(±1.50)	101.02(±5.02)
cow milk	-	5	4.31(±0.17)	86.23(±3.48)
	-	100	103.6(±3.09)	103.6(±3.09)

[a] Supporting electrolyte: phosphate buffer saline (pH 7.0).

DPV outcomes. In this sense, these parameters were studied according to Table S1. The DPV measurements and the dot plot are shown in Figure S4.

With the study of the effects of the parameters concluded, using the DPV with a modulation amplitude of 0.09 V, an interval time of 0.005 V s^{-1} and a modulation time of 0.08 s an analytical curve was performed. Studies were performed in a phosphate buffer solution (pH 7.0). Then, the analytical performance of the CBSP-PVP-CH/PES was investigated by successive and crescent concentrations of TRP additions (Figure 7C). The analytical curve was obtained in a linear range (R^2 = 0.9946) from 0.5 to 300 μmol L^{-1}, following eq 3 (Figure 7D)

$$I(\mu A) = 0.0056[TRP] - 1.235 \times 10^{-8} \quad (3)$$

The limit of detection (LOD) and the limit of quantification (LOQ) were determined by calculating three and ten times the standard deviation of the intercept, respectively, divided by the slope of the calibration plot [28]. The resulting LOD value was determined to be 0.018 μmol L^{-1}, and the LOQ value was established at 0.060 μmol L^{-1}.

The TRP determination was also performed in TRP pharmaceutical (tablets) and spiked beverages (apple juice and cow milk). Table 1 shows the added and found TRP concentrations and the recovery values for the respective samples. It was possible to find recovery values from 86.2 to 114% considering all evaluated samples. This demonstrates that the proposed method was also successful in TRP determination in different samples.

For interference study (Figure 8), DPV measurements were performed for the presence of concomitant species, Ascorbic Acid (AA), L-lysine (L-lys), Melatonin (MLT), Serotonin (STN), and Uric Acid (UA) at the same concentration (100 mmol L^{-1}). The interference percentages were between 2.08 and 9.15% showing the functionality of this sensor.

Table 2 compares the analytical characteristics of the SPE sensor developed with a water-based CBSP ink for the diagnosis of tryptophan with other previously reported sensors.[61−67] The selected studies have similarities with the proposed electrode, such as using carbon materials and the disposable approach. Due to the simplicity of the manufacturing process for the water-based conductive ink, the CBSP-PVP-CH/PES electrodes, and the affordable cost of the materials used, the analytical performance of the proposed sensor is remarkably satisfactory and is characterized by its linear ranges and limits of detection (LODs).

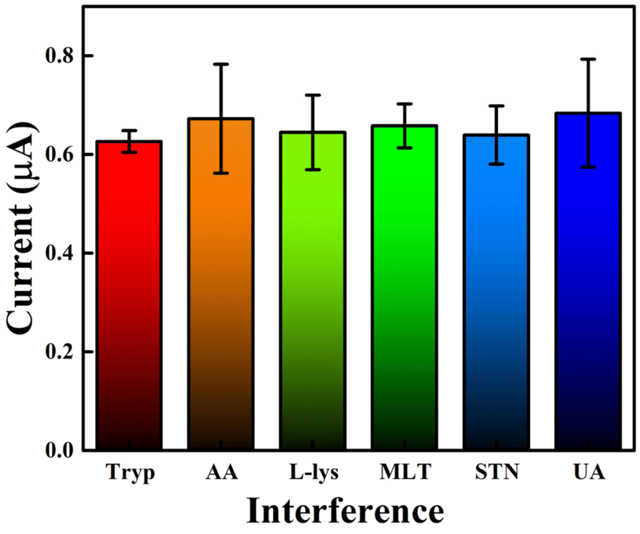

Figure 8. Results obtained (%) for interference study using different species for TRP determination. Supporting electrolyte: phosphate buffer saline (pH 7.0).

4. ANALYTICAL GREENNESS METRIC (AGREE)

The AGREE metric comprehensively assesses the environmental friendliness of analytical approaches by ranking proposed and reported methods based on the 12 principles of Green Analytical Chemistry (GAC).[68] This tool is a user-friendly application that generates a simple, visually appealing pictogram by analyzing 12 input variables for each method. Each pictogram consists of 12 radial sectors, ranging in color from forest green to red, and a central score indicating the overall performance.[69] The final score ranges from zero to one, with values closer to one representing a greener method.[69] Using the AGREE model, our proposed method achieved a superior score of 0.83, due to the use of water—a naturally abundant, nontoxic, sustainable and environmentally friendly solvent, see Figure 9.

5. CONCLUSIONS

In conclusion, the development of electrochemical sensors has made significant progress, driven by the demand for versatile, cost-effective and reproducible devices. In this context, sustainability has emerged as a key priority, affecting material selection and manufacturing techniques. This article describes the development of an SPE sensor using an environmentally friendly water-based CBSP ink for the diagnosis of tryptophan. The use of a sustainable, nontoxic ink formulation emphasizes the green chemistry approach taken in this work, reducing the environmental impact associated with conventional sensor

Table 2. Analytical Performance of the CBSP-PVP-CH/PES for Tryptophan Determination Compared with the Literature[a]

electrode	technique	LDR (mol L^{-1})	LOD (mol L^{-1})	samples	ref
QDs/GA/PPD/SPCE	SWV	100.0−500.0	14.74	beverage	61
SPCE/GO−COOH/Chitosan sensor	DPV	0.4−40.0	0.1	milk	62
SPE/rGO/AuNPs	DPV	0.5−500.0	0.39	human plasma, serum and saliva	63
Fe_3O_4@SiO_2/GO/SPE	DPV	1.0−400.0	0.2	human blood serum and urine	64
BCN-SPE	DPV	1.0−400.0	0.036	egg white and human urine	65
3:1gCN.Meth|SPE	SWV	1.0−60 and 60−300	0.029	oats, pumpkin, kidney beans and pharmaceutical	66
PdCuCo/RGO/SPCE	DPV	0.08−20.0	0.03	plasma	67
CBSP-PVP-CH/PES	DPV	0.5−300.0	0.018	pharmaceutical and beverage	this work

[a] **QDs/GA/PPD/SPCE**: Poly(p-phenylenediamine) polymer film/cysteamine capped cadmium sulfide quantum dots over a screen-printed carbon electrode; **SPCE/GO−COOH/Chitosan sensor**: Modified Screen-Printed Carbon Electrode (SPCE) with Graphene Oxide−COOH/Chitosan electrodeposited; **SPE/rGO/AuNPs**: Screen-printed electrode modified with a reduced graphene oxide/gold nanoparticles; **Fe3O4@SiO2/GO/SPE**: Core−shell Fe3O4@SiO2/GO nanocomposite modified graphite screen printed electrode; **BCN-SPE**: boron carbon nitride (BCN)-assisted SPE surface functionalization; **3:1 gCN.Meth|SPE**: poly methionine/graphitic carbon nitride modified screen-printed electrode; **PdCuCo/RGO/SPCE**: screen-printed electrode modified with PdCuCo ternary NPs and reduced graphene oxide.

Figure 9. AGREE score for CBSP-PVP-CH/PES in the detection of tryptophan.

manufacture. Subsequently, the analytical performance of the CBSP-PVP-CH/PES was investigated by successive and crescent addition of TRP concentrations. The analytical curve was obtained in a linear range (R^2 = 0.9946) from 0.5 to 300 μmol L^{-1}, following eq 3: I (μA) = 0.0056 [TRP] − 1.235 × 10^{-8}, with LOD 0.018 μmol L^{-1} and LOQ 0.060 μmol L^{-1}. Interference studies proved the functionality of the sensor with interference percentages between 2.08 and 9.15% for different companion species. The sensor enabled the successful determination of tryptophan concentration in pharmaceutical tablets and spiked beverages, with recovery rates ranging from 86.2% to 114%. The environmentally conscious design combined with the excellent analytical performance makes the proposed sensor a sustainable and efficient tool for the determination of tryptophan in various sample matrices.

■ ASSOCIATED CONTENT

Data Availability Statement

The data will be available under requirement.

Supporting Information

The Supporting Information is available free of charge at https://pubs.acs.org/doi/10.1021/acsaelm.5c00550.

> Electrochemical characterization of CBSP electrodes; reproducibility tests with varying squeegee passes; scan rate studies with ferrocenemethanol; optimization of DPV parameters for TRP detection, a summary table highlighting the effects of experimental parameters on the current response; contact angle measurements; FTIR and EIS analyses; selectivity and stability assessments (PDF)

■ AUTHOR INFORMATION

Corresponding Authors

Bruno C. Janegitz − *Laboratory of Sensors, Nanomedicine and Nanostructured Materials, Federal University of São Carlos, Araras 13600-970, Brazil;* orcid.org/0000-0001-9707-9795; Email: brunocj@ufscar.br

Craig E. Banks − *Faculty of Science and Engineering, Manchester Metropolitan University, Manchester M1 5GD, Great Britain;* orcid.org/0000-0002-0756-9764; Email: c.banks@mmu.ac.uk

Authors

Jéssica R Camargo − *Faculty of Science and Engineering, Manchester Metropolitan University, Manchester M1 5GD, Great Britain; Laboratory of Sensors, Nanomedicine and Nanostructured Materials, Federal University of São Carlos, Araras 13600-970, Brazil;* orcid.org/0000-0003-1836-7495

Robert D. Crapnell − *Faculty of Science and Engineering, Manchester Metropolitan University, Manchester M1 5GD, Great Britain;* orcid.org/0000-0002-8701-3933

Elena Bernalte − *Faculty of Science and Engineering, Manchester Metropolitan University, Manchester M1 5GD, Great Britain*

Complete contact information is available at: https://pubs.acs.org/10.1021/acsaelm.5c00550

Author Contributions

J.R.C.: Writing—review and editing, writing—original draft, methodology, investigation, formal analysis, data curation. R.D.C.: Writing —review and editing, writing—original draft, supervision, methodology, investigation, formal analysis, data curation, conceptualization. E.B.: Writing—review and editing, writing—original draft, supervision, methodology, investigation, formal analysis, data curation, conceptualization. B.C.J.: Writing—review and editing, writing—original draft, supervision, methodology, investigation, funding acquisition. C.E.B.: Writing—review and editing, writing—original draft, supervision, resources, project administration, methodology, investigation, funding acquisition, formal analysis, data curation, conceptualization.

Funding

The Article Processing Charge for the publication of this research was funded by the Coordenacao de Aperfeicoamento de Pessoal de Nivel Superior (CAPES), Brazil (ROR identifier: 00x0ma614).

Notes

The authors declare no competing financial interest.

ACKNOWLEDGMENTS

We gratefully acknowledge the Brazilian funding agencies: São Paulo Research Foundation (FAPESP, grant# 2023/00321-3, grant# 2019/23177-0, and grant# 2023/06793-4), National Council for Scientific and Technological Development (CNPq), Funding Authority for Studies and Projects (FINEP, grant# 01.22.0179.00, project MARTMA), and Brazilian Federal Agency for Support and Evaluation of Graduate Education (CAPES, 001 and grant# 88887.986513/2024-00).

REFERENCES

(1) Umapathi, R.; Ghoreishian, S. M.; Sonwal, S.; Rani, G. M.; Huh, Y. S. Portable electrochemical sensing methodologies for on-site detection of pesticide residues in fruits and vegetables. *Coord. Chem. Rev.* **2022**, *453*, No. 214305.

(2) Turner, A. P. F. Biosensors: sense and sensibility. *Chem. Soc. Rev.* **2013**, *42* (8), 3184−3196.

(3) Dias, A. A.; Chagas, C. L. S.; Silva-Neto, H. d. A.; Lobo-Junior, E. O.; Sgobbi, L. F.; de Araujo, W. R.; Paixão, T. R. L. C.; Coltro, W. K. T. Environmentally friendly manufacturing of flexible graphite electrodes for a wearable device monitoring zinc in sweat. *ACS Appl. Mater. Interfaces* **2019**, *11* (43), 39484−39492.

(4) Niculescu, A.-G.; Chircov, C.; Bîrcă, A. C.; Grumezescu, A. M. Fabrication and applications of microfluidic devices: A review. *Int. J. Mol. Sci.* **2021**, *22* (4), No. 2011.

(5) Campuzano, S.; Pedrero, M.; Yáñez-Sedeño, P.; Pingarrón, J. M. New challenges in point of care electrochemical detection of clinical biomarkers. *Sens. Actuators, B* **2021**, *345*, No. 130349.

(6) Crapnell, R. D.; Banks, C. E. Electroanalytical Overview: Screen-Printed Electrochemical Sensing Platforms. *ChemElectroChem* **2024**, *11* (19), No. e202400370.

(7) de Oliveira, P. R.; de Freitas, R. C.; de Souza Carvalho, J. H.; Camargo, J. R.; Guterres e Silva, L. R.; Janegitz, B. C. Overcoming disposable sensors pollution: Using of circular economy in electrodes application. *Curr. Opin. Environ. Sci. Health* **2024**, *38*, No. 100540.

(8) United Nations. The 17 sustainable development goals. https://sdgs.un.org/goals.

(9) Lakhera, P.; Chaudhary, V.; Jha, A.; Singh, R.; Kush, P.; Kumar, P. Recent developments and fabrication of the different electrochemical biosensors based on modified screen printed and glassy carbon electrodes for the early diagnosis of diverse breast cancer biomarkers. *Mater. Today Chem.* **2022**, *26*, No. 101129.

(10) Li, M.; Li, D.-W.; Xiu, G.; Long, Y.-T. Applications of screen-printed electrodes in current environmental analysis. *Curr. Opin. Electrochem.* **2017**, *3* (1), 137−143.

(11) Fava, E. L.; do Prado, T. M.; Garcia-Filho, A.; Silva, T. A.; Cincotto, F. H.; de Moraes, F. C.; Faria, R. C.; Fatibello-Filho, O. Non-enzymatic electrochemical determination of creatinine using a novel screen-printed microcell. *Talanta* **2020**, *207*, No. 120277.

(12) Paschoalin, R. T.; Gomes, N. O.; Almeida, G. F.; Bilatto, S.; Farinas, C. S.; Machado, S. A. S.; Mattoso, L. H. C.; Oliveira, O. N., Jr.; Raymundo-Pereira, P. A. Wearable sensors made with solution-blow spinning poly (lactic acid) for non-enzymatic pesticide detection in agriculture and food safety. *Biosens. Bioelectron.* **2022**, *199*, No. 113875.

(13) Singh, S.; Wang, J.; Cinti, S. An Overview on Recent Progress in Screen-Printed Electroanalytical (Bio) Sensors. *ECS Sens. Plus* **2022**, *1*, No. 023401.

(14) Oliveira, A.; Pereira, A.; Resende, M. Fabrication of low-cost screen-printed electrode in paper using conductive inks of graphite and silver/silver chloride. *Electroanalysis* **2023**, *35*, No. e202200093, DOI: 10.1002/elan.202200093.

(15) Pavličková, M.; Lorencová, L.; Hatala, M.; Kováč, M.; Tkáč, J.; Gemeiner, P. Facile fabrication of screen-printed MoS2 electrodes for electrochemical sensing of dopamine. *Sci. Rep.* **2022**, *12* (1), No. 11900.

(16) Palley, B. F.; Artur, J. C.; De Arruda, M. N.; De Souza, G. F.; Graves, D. A.; de Carvalho Bovolato, A. L.; Deffune, E.; Schelp, A. O.; Gonçalves, E. S.; De Moraes, M. L. Screen-Printed Electrodes on Tyvek Substrate as Low-Cost Device to Applications in Alzheimer's Disease Detection. *J. Electrochem. Soc.* **2022**, *169* (3), No. 037505.

(17) Zhang, Z.; Tian, B.; Li, L.; Lei, J.; Liu, Z.; Liu, J.; Cheng, G.; Zhao, N.; Fang, X.; Zhao, L. J. C. I. Thermoelectricity and antivibration properties of screen-printed nanodoped In1. 35ZnO2. 11/In2O3 thin-film thermocouples on alumina substrates. *Ceram. Int.* **2022**, *48* (18), 25747−25755, DOI: 10.1016/j.ceramint.2022.05.246.

(18) Sher, M.; Faheem, A.; Asghar, W.; Cinti, S. Nano-engineered screen-printed electrodes: A dynamic tool for detection of viruses. *TrAC, Trends Anal. Chem.* **2021**, *143*, No. 116374.

(19) Huang, L.; Huang, Y.; Liang, J.; Wan, X.; Chen, Y. Graphene-based conducting inks for direct inkjet printing of flexible conductive patterns and their applications in electric circuits and chemical sensors. *Nano Res.* **2011**, *4* (7), 675−684.

(20) Camargo, J. R.; Orzari, L. O.; Araújo, D. A. G.; de Oliveira, P. R.; Kalinke, C.; Rocha, D. P.; dos Santos, A. L.; Takeuchi, R. M.; Munoz, R. A. A.; Bonacin, J. A.; Janegitz, B. C. Development of conductive inks for electrochemical sensors and biosensors. *Microchem. J.* **2021**, *164*, No. 105998.

(21) Kamarudin, S. F.; Mustapha, M.; Kim, J.-K. Green strategies to printed sensors for healthcare applications. *Polym. Rev.* **2021**, *61* (1), 116−156.

(22) Ikram, R.; Jan, B. M.; Qadir, M. A.; Sidek, A.; Stylianakis, M. M.; Kenanakis, G. Recent advances in chitin and chitosan/graphene-based bio-nanocomposites for energetic applications. *Polymers* **2021**, *13* (19), No. 3266.

(23) Carrera, C.; Bengoechea, C.; Carrillo, F.; Calero, N. Effect of deacetylation degree and molecular weight on surface properties of chitosan obtained from biowastes. *Food Hydrocolloids* **2023**, *137*, No. 108383.

(24) Jochelavicius, K.; Pereira, A. R.; Fiamingo, A.; Nobre, T. M.; Campana-Filho, S. P.; Oliveira, O. N., Jr. Chitosan effects on monolayers of zwitterionic, anionic and a natural lipid extract from *E. coli* at physiological pH. *Colloids Surf., B* **2022**, *209*, No. 112146.

(25) Zhang, J.; Li, C. M. Nanoporous metals: fabrication strategies and advanced electrochemical applications in catalysis, sensing and energy systems. *Chem. Soc. Rev.* **2012**, *41* (21), 7016−7031.

(26) Chen, D.; Feng, H.; Li, J. Graphene oxide: preparation, functionalization, and electrochemical applications. *Chem. Rev.* **2012**, *112* (11), 6027−6053.

(27) de Araujo Andreotti, I. A.; Orzari, L. O.; Camargo, J. R.; Faria, R. C.; Marcolino-Junior, L. H.; Bergamini, M. F.; Gatti, A.; Janegitz, B. C. Disposable and flexible electrochemical sensor made by recyclable material and low cost conductive ink. *J. Electroanal. Chem.* **2019**, *840*, 109−116.

(28) Saidina, D. S.; Eawwiboonthanakit, N.; Mariatti, M.; Fontana, S.; Hérold, C. Recent development of graphene-based ink and other conductive material-based inks for flexible electronics. *J. Electron. Mater.* **2019**, *48* (6), 3428−3450.

(29) Liu, L.; Shen, Z.; Zhang, X.; Ma, H. Highly conductive graphene/carbon black screen printing inks for flexible electronics. *J. Colloid Interface Sci.* **2021**, *582*, 12−21.

(30) Fan, Z.; Tong, W.; Luo, G.; Wei, F. Fabrication and characterization of multi-walled carbon nanotubes-based ink. *J. Mater. Sci.* **2005**, *40* (18), 5075−5077.

(31) Jafari, S.; Burr, L.; Migliorelli, D.; Galve, R.; Marco, M. P.; Campbell, K.; Elliott, C.; Suman, M.; Sturla, S. J.; Generelli, S. Smartphone-based magneto-immunosensor on carbon black modified screen-printed electrodes for point-of-need detection of aflatoxin B1 in cereals. *Anal. Chim. Acta* **2022**, *1221*, No. 340118.

(32) Nelis, J. L. D.; Migliorelli, D.; Jafari, S.; Generelli, S.; Lou-Franco, J.; Salvador, J. P.; Marco, M. P.; Cao, C.; Elliott, C. T.; Campbell, K. The benefits of carbon black, gold and magnetic nanomaterials for point-of-harvest electrochemical quantification of domoic acid. *Microchim. Acta* **2020**, *187* (3), No. 164.

(33) Nelis, J. L. D.; Migliorelli, D.; Mühlebach, L.; Generelli, S.; Stewart, L.; Elliott, C. T.; Campbell, K. Highly sensitive electrochemical detection of the marine toxins okadaic acid and domoic acid with carbon black modified screen printed electrodes. *Talanta* **2021**, *228*, No. 122215.

(34) Cho, I.; Choi, J.; Kim, K.; Ryou, M.-H.; Lee, Y. M. J. R. A. A comparative investigation of carbon black (Super-P) and vapor-grown carbon fibers (VGCFs) as conductive additives for lithium-ion battery cathodes. *RSC Adv.* **2015**, *5* (115), 95073−95078.

(35) Veloso, W. B.; Almeida, A. T. D. F. O.; Ribeiro, L. K.; de Assis, M.; Longo, E.; Garcia, M. A. S.; Tanaka, A. A.; da Silva, I. S.; Dantas, L. M. F. Rapid and sensitivity determination of macrolides antibiotics using disposable electrochemical sensor based on Super P carbon black and chitosan composite. *Microchem. J.* **2022**, *172*, No. 106939.

(36) Wu, L.; Shi, X.; Wu, Z. S. Recent advancements and perspectives of biodegradable polymers for supercapacitors. *Adv. Funct. Mater.* **2023**, *33* (16), No. 2211454.

(37) Henrique, J. M.; Camargo, J. R.; de Oliveira, G. G.; Stefano, J. S.; Janegitz, B. C. Disposable electrochemical sensor based on shellac and graphite for sulfamethoxazole detection. *Microchem. J.* **2021**, *170*, No. 106701.

(38) Freitas, R. C.; Orzari, L. O.; Ferreira, L. M. C.; Paixão, T. R. L. C.; Coltro, W. K. T.; Vicentini, F. C.; Janegitz, B. C. Electrochemical determination of melatonin using disposable self-adhesive inked paper electrode. *J. Electroanal. Chem.* **2021**, *897*, No. 115550.

(39) Camargo, J. R.; Silva, T. A.; Rivas, G. A.; Janegitz, B. C. Novel eco-friendly water-based conductive ink for the preparation of disposable screen-printed electrodes for sensing and biosensing applications. *Electrochim. Acta* **2022**, *409*, No. 139968.

(40) Pradela-Filho, L. A.; Andreotti, I. A. A.; Carvalho, J. H. S.; Araujo, D. A. G.; Orzari, L. O.; Gatti, A.; Takeuchi, R. M.; Santos, A. L.; Janegitz, B. C. Glass varnish-based carbon conductive ink: A new way to produce disposable electrochemical sensors. *Sens. Actuators, B* **2020**, *305*, No. 127433.

(41) Daniele, G. G.; de Souza, D. C.; de Oliveira, P. R.; Orzari, L. O.; Blasques, R. V.; Germscheidt, R. L.; da Silva, E. C.; Pocrifka, L. A.; Bonacin, J. A.; Janegitz, B. C. Development of Disposable and Flexible Supercapacitor Based on Carbonaceous and Ecofriendly Materials. *C* **2022**, *8* (2), No. 32.

(42) Raymundo-Pereira, P. A.; Gomes, N. O.; Carvalho, J. H. S.; Machado, S. A. S.; Oliveira, O. N., Jr.; Janegitz, B. C. Simultaneous detection of quercetin and carbendazim in wine samples using disposable electrochemical sensors. *ChemElectroChem* **2020**, *7* (14), 3074−3081.

(43) Phillips, C.; Al-Ahmadi, A.; Potts, S.-J.; Claypole, T.; Deganello, D. The effect of graphite and carbon black ratios on conductive ink performance. *J. Mater. Sci.* **2017**, *52* (16), 9520−9530.

(44) Pandhi, T.; Cornwell, C.; Fujimoto, K.; Barnes, P.; Cox, J.; Xiong, H.; Davis, P. H.; Subbaraman, H.; Koehne, J. E.; Estrada, D. Fully inkjet-printed multilayered graphene-based flexible electrodes for repeatable electrochemical response. *RSC Adv.* **2020**, *10* (63), 38205−38219.

(45) Delgado-Andrade, C.; Rufián-Henares, J. A.; Jiménez-Pérez, S.; Morales, F. J. Tryptophan determination in milk-based ingredients and dried sport supplements by liquid chromatography with fluorescence detection. *Food Chem.* **2006**, *98* (3), 580−585.

(46) Badawy, A.-B. Plasma free tryptophan revisited: what you need to know and do before measuring it. *J. Psychopharmacol.* **2010**, *24* (6), 809−815.

(47) Dinu, A.; Apetrei, C. A Review of Sensors and Biosensors Modified with Conducting Polymers and Molecularly Imprinted Polymers Used in Electrochemical Detection of Amino Acids: Phenylalanine, Tyrosine, and Tryptophan. *Int. J. Mol. Sci.* **2022**, *23* (3), No. 1218.

(48) Gecse, K.; Dobos, D.; Aranyi, C. S.; Galambos, A.; Baksa, D.; Kocsel, N.; Szabó, E.; Pap, D.; Virág, D.; Ludányi, K.; et al. Association of plasma tryptophan concentration with periaqueductal gray matter functional connectivity in migraine patients. *Sci. Rep.* **2022**, *12* (1), No. 739.

(49) Bech-Andersen, S. Determination of Tryptophan with HPLC after Alkaline Hydrolysis in Autoclave using α-methyl-tryptophan as Internal Standard. *Acta Agric. Scand.* **1991**, *41* (3), 305−309.

(50) La Cour, R.; Jørgensen, H.; Schjoerring, J. K. Improvement of tryptophan analysis by liquid chromatography-single quadrupole mass spectrometry through the evaluation of multiple parameters. *Front. Chem.* **2019**, *7*, No. 797.

(51) Hanaoka, S.; Lin, J.-M.; Yamada, M. Chemiluminescence behavior of the decomposition of hydrogen peroxide catalyzed by copper (II)−amino acid complexes and its application to the determination of tryptophan and phenylalanine. *Anal. Chim. Acta* **2000**, *409* (1−2), 65−73.

(52) da Silva, V. A. O. P.; Tartare, V. A. P.; Kalinke, C.; Oliveira, P. R.; Souza, D. C.; Bonacin, J. A.; Janegitz, B. C. Lab-made 3D-printed contact angle measurement adjustable holder. *Quim. Nova* **2020**, *43* (9), 1312−1319.

(53) Whittingham, M. J.; Hurst, N. J.; Crapnell, R. D.; Ferrari, A. G.-M.; Blanco, E.; Davies, T. J.; Banks, C. E. Electrochemical improvements can be realized via shortening the length of screen-printed electrochemical platforms. *Anal. Chem.* **2021**, *93* (49), 16481−16488.

(54) Costa, S.; Borowiak-Palen, E.; Kruszynska, M.; Bachmatiuk, A.; Kalenczuk, R. J. Characterization of carbon nanotubes by Raman spectroscopy. *Mater. Sci.-Pol.* **2008**, *26* (2), 433−441.

(55) Poukhovoi, A.; Schipporeit, S.; Becker, H. W.; Calliari, L.; Buck, V. Assessment of spectroscopic methods for the characterisation of DLC films deposited by PECVD. *J. Optoelectron. Adv. Mater.* **2012**, *14* (3-4), 383−392.

(56) Poonguzhali, R.; Basha, S. K.; Kumari, V. S. Synthesis and characterization of chitosan-PVP-nanocellulose composites for in-vitro wound dressing application. *Int. J. Biol. Macromol.* **2017**, *105*, 111−120.

(57) Jiao, X.; Xie, J.; Hao, M.; Li, Y.; Wang, C.; Zhu, Z.; Wen, Y. Chitosan Biguanidine/PVP Antibacterial Coatings for Perishable Fruits. *Polymers* **2022**, *14*, No. 2704, DOI: 10.3390/polym14132704.

(58) Grant, J. J.; Pillai, S. C.; Perova, T. S.; Hehir, S.; Hinder, S. J.; McAfee, M.; Breen, A. Electrospun Fibres of Chitosan/PVP for the Effective Chemotherapeutic Drug Delivery of 5-Fluorouracil. *Chemosensors* **2021**, *9*, No. 70, DOI: 10.3390/chemosensors9040070.

(59) Ferrari, A. G.-M.; Foster, C. W.; Kelly, P. J.; Brownson, D. A. C.; Banks, C. E. Determination of the electrochemical area of screen-printed electrochemical sensing platforms. *Biosensors* **2018**, *8* (2), No. 53.

(60) PubChem Compound Summary for CID 6305,Tryptophan. https://pubchem.ncbi.nlm.nih.gov/compound/Tryptophan. (accessed May 12).

(61) Boonchiangma, S.; Srijaranai, S.; Tuntulani, T.; Ngeontae, W. A highly selective electrochemical sensor for l-tryptophan based on a screen-printed carbon electrode modified with poly-p-phenylenediamine and CdS quantum dots *J. Appl. Polym. Sci.* 2014; Vol. *131* 11 DOI: 10.1002/app.40356.

(62) Fooladi, E.; Razavizadeh, B. M.; Noori, M.; Kakooei, S. Application of carboxylic acid-functionalized of graphene oxide for electrochemical simultaneous determination of tryptophan and tyrosine in milk. *SN Appl. Sci.* **2020**, *2* (4), No. 527.

(63) Nazarpour, S.; Hajian, R.; Sabzvari, M. H. A novel nanocomposite electrochemical sensor based on green synthesis of reduced graphene oxide/gold nanoparticles modified screen printed electrode for determination of tryptophan using response surface methodology approach. *Microchem. J.* **2020**, *154*, No. 104634.

(64) Beitollahi, H.; Safaei, M.; Shishehbore, M. R.; Tajik, S. Application of Fe3O4@ SiO2/GO nanocomposite for sensitive and selective electrochemical sensing of tryptophan. *J. Electrochem. Sci. Eng.* **2018**, *9* (1), 45−53.

(65) Garg, S.; Singh, A.; Parmar, A. S.; Rosy. Boron Carbon Nitride-Assisted Electro-Functionalization of Screen-Printed Electrode for Tryptophan Sensing. *ACS Appl. Nano Mater.* **2023**, *6* (16), 14849−14860.

(66) Singh, A. K.; Yadav, R.; Singh, A.; Rosy. Poly-methionine/graphitic carbon nitride modified screen-printed electrodes: A metal-free, bio-interface for tryptophan sensing. *Mater. Chem. Phys.* **2024**, *328*, No. 129941.

(67) Khoshsafar, H.; Bagheri, H.; Hashemi, P.; Bordbar, M. M.; Madrakian, T.; Afkhami, A. Combination of an aptamer-based immunochromatography assay with nanocomposite-modified screen-printed electrodes for discrimination and simultaneous determination of tryptophan enantiomers. *Talanta* **2023**, *253*, No. 124090.

(68) Gałuszka, A.; Migaszewski, Z.; Namieśnik, J. The 12 principles of green analytical chemistry and the SIGNIFICANCE mnemonic of green analytical practices. *TrAC, Trends Anal. Chem.* **2013**, *50*, 78−84.

(69) Mohyeldin, S. M.; Daabees, H. G.; Talaat, W.; Kamal, M. F. AGREE, hexagonal and whiteness assessment approaches for evaluating two novel analytical methods; capillary zone electrophoresis and spectrophotometric assays for simultaneous determination of pantoprazole, chlordiazepoxide, and clidinium bromide ternary mixtures. *Sustainable Chem. Pharm.* **2023**, *33*, No. 101108.